provided by University of East Anglia digital r

Wave Motion ▮ (▮▮▮▮) ▮▮▮–▮▮▮

Contents lists available at ScienceDirect

Wave Motion

journal homepage: www.elsevier.com/locate/wavemoti

Numerical and asymptotic solutions of generalised Burgers' equation

J.M. Schofield *, P.W. Hammerton

School of Mathematics, University of East Anglia, Norwich NR4 7TJ, UK

HIGHLIGHTS

- We generate a numerical scheme to solve Burgers' equation using a variable mesh scheme.
- We validate asymptotic prediction for shock location and width for small times.
- Show partial breakdown in spherical case from a tanh shock to an erf shock.
- Offers validation of Enflo's old age form for cylindrical case.

ARTICLE INFO

Article history:
Received 18 October 2013
Received in revised form 28 January 2014
Accepted 25 March 2014
Available online xxxx

Keywords:
Generalised Burgers' equation
Nonlinear acoustics
Shock waves

ABSTRACT

The generalised Burgers' equation models the nonlinear evolution of acoustic disturbances subject to thermoviscous dissipation. When thermoviscous effects are small, asymptotic analysis predicts the development of a narrow shock region, which widens, leading eventually to a shock-free linear decay regime. The exact nature of the evolution differs subtly depending upon whether plane waves are considered, or cylindrical or spherical spreading waves. This paper focuses on the differences in asymptotic shock structure and validates the asymptotic predictions by comparison with numerical solutions. Precise expressions for the shock width and shock location are also obtained.

© 2014 Elsevier B.V. All rights reserved.

1. Introduction

When studying the propagation of sonic booms through the atmosphere, the shock amplitude and shock width (or equivalently shock rise-time) are the quantities of most interest, especially when considering the annoyance and potential damage associated with such shocks. Initially, model equations with one spatial dimension were studied taking account of the combined effect of nonlinear steepening and thermoviscous diffusion [1]. This simple model was then extended to take account of geometric spreading [2] with justification that these model governing equations form a rational approximation to the full equations of fluid motion. Further studies include the effect of atmospheric stratification [3], other dissipation mechanisms such as molecular relaxation [4,5] or combinations of all these effects [6,7]. Alongside these investigations, numerical studies typically involved either direct solution of model equations [8,9] or separation of nonlinear terms from linear frequency-dependent terms [10–13].

For the physical parameter ranges of most interest, the shock width is small compared to the overall wavelength and the need for a good estimate of the shock width leads to the need for fine spatial resolution. Moreover, it is found that in some regimes the shock width is sensitive to small changes in material parameters. A numerical solution, while identifying such changes, does little to highlight which physical processes are of key importance. For these reasons, asymptotic analysis

* Corresponding author. Tel.: +44 7969775683.
E-mail address: j.schofield@uea.ac.uk (J.M. Schofield).

http://dx.doi.org/10.1016/j.wavemoti.2014.03.005
0165-2125/© 2014 Elsevier B.V. All rights reserved.

Please cite this article in press as: J.M. Schofield, P.W. Hammerton, Numerical and asymptotic solutions of generalised Burgers' equation, Wave Motion (2014), http://dx.doi.org/10.1016/j.wavemoti.2014.03.005

making use of the disparity in spatial scales is a useful approach. In the case of wave disturbances spreading with cylindrical or spherical symmetry, Crighton and Scott [14] chart the variation of the shock width, along with the internal shock structure, up to a stage at which the evolution is linear and shock-free (the so-called old-age solution). Such an approach, while very intricate, is valuable in that it reveals the time scales at which qualitative changes in the solution occur. Similar approaches have also been taken when the thermoviscous diffusion is supplemented by relaxation effects associated with polyatomic molecules, revealing intricate variation in the finest shock scale [6,15]. However, up to this point the asymptotic predictions have never been fully validated.

The ultimate aim of any study of propagation of sonic booms through the atmosphere, with given meteorological data, is to predict shock properties such as amplitude and rise-time at the ground and identify what physical properties control these quantities. As previously noted, direct numerical solutions can be computationally expensive, but more importantly do not necessarily identify the key physical parameter regimes. For this reason, asymptotic analysis undoubtedly has a role to play in understanding the propagation of sonic booms through real atmospheres. However, first a rigorous validation of asymptotic results for simpler systems is required, and this is the primary motivation for the present work.

When studying finite amplitude plane acoustic waves propagating through a thermoviscous medium, Mendousse [1] introduced Burgers' equation in the form

$$\frac{\partial v}{\partial x} - v\frac{\partial v}{\partial \theta} = \nu\frac{\partial^2 v}{\partial \theta^2}, \qquad v(x_0, \theta) = f(\theta)$$

where ν is the viscosity and v represents either particle displacement velocity or perturbation pressure, θ is a retarded time and x is propagation distance. An alternative form,

$$\frac{\partial v}{\partial t} + v\frac{\partial v}{\partial x'} = \nu\frac{\partial^2 v}{\partial x'^2}, \qquad v(x', t_0) = \phi(x') \tag{1}$$

is more appropriate for the corresponding initial value problem, with x' the spatial coordinate in the frame moving with the linear sound speed. In each of these forms, quadratic nonlinearity and thermoviscous diffusion act to modify a disturbance travelling at the linear sound speed. By means of a nonlinear transformation [16,17], Burgers' equation can be transformed to the heat equation and hence solved for arbitrary initial conditions. This solution is commonly referred to as the Cole–Hopf solution and, for the plane Burgers' equation (1), can be written as [18]

$$v(x', t) = \frac{1}{t}\frac{\int_{-\infty}^{\infty}(x' - X)\psi(x', X, t)dX}{\int_{-\infty}^{\infty}\psi(x', X, t)dX},$$

where

$$\psi(x', X, t) = \exp\left[-\frac{1}{2\nu}\left(\frac{(x' - X)^2}{2t} + \int_0^X \phi(s)ds\right)\right].$$

The fact that an exact solution exists means that the plane Burgers' equation has been much studied as a test case for numerical methods of solving nonlinear wave equations [19,20].

Subsequently, the formal validity of Burgers' equation as a model for nonlinear acoustics was investigated [2,21]. Extending to a right/outward travelling sound wave which has planar, cylindrical or spherical symmetry [2] and using the notation that all starred variables are dimensional, the equation governing the perturbation velocity of the medium is given by

$$\frac{\partial u^*}{\partial t^*} + \frac{\gamma + 1}{2}u^*\frac{\partial u^*}{\partial X^*} + j\frac{u^*}{2t^*} = \frac{1}{2}\Delta\frac{\partial^2 u^*}{\partial X^{*2}}, \qquad X^* = r^* - a_0 t^*. \tag{2}$$

Here γ is the adiabatic exponent, a_0 is the small-signal sound speed, r^* is the radial propagation distance, Δ is the diffusivity of sound and $j = 0, 1, 2$ for plane, cylindrical and spherical waves respectively. For a disturbance of typical wavelength l^*, this equation can be derived formally using a multiple scales argument [21], based on the assumptions that:

(i) finite amplitude effects are locally small ($u^*/a_0 \ll 1$);
(ii) geometric spreading effects are small ($l^*/r^* \ll 1$);
(iii) thermoviscous diffusive effects are small ($\Delta/a_0 l^* \ll 1$).

This paper is concerned with the physically important case when thermoviscous effects are smaller than nonlinear effects over most of the waveform. However, in order to analyse the structure of the solution in the three cases of planar, cylindrical and spherical spreading it proves most convenient to apply the transformation described in Crighton and Scott [14] (equations (2.3–2.5)). This converts the geometric spreading term into a range dependent viscosity term, leading to the generalised Burgers' equation (GBE),

$$\frac{\partial U}{\partial T} + U\frac{\partial U}{\partial X} = \epsilon G(T)\frac{\partial^2 U}{\partial X^2}, \tag{3}$$

Please cite this article in press as: J.M. Schofield, P.W. Hammerton, Numerical and asymptotic solutions of generalised Burgers' equation, Wave Motion (2014), http://dx.doi.org/10.1016/j.wavemoti.2014.03.005

with initial condition $U(X, 1) = U_0(X)$. Here ϵ can be considered an inverse Reynolds number (or non-dimensional viscosity) and

$$G(T) = \begin{cases} 1, & \text{Plane;} \\ \frac{1}{2}(T + T_0 - 1), & \text{Cylindrical;} \\ \exp\left(\frac{T}{T_0}\right), & \text{Spherical.} \end{cases} \tag{4}$$

For the cylindrical and spherical cases, T_0 is a non-dimensional parameter related to the scalings at the initial time, the exact definition of which [14] is not important for the present study. For algebraic simplicity we set $T_0 = 1$, though the analysis can be readily extended to T_0 being an arbitrary $O(1)$ constant.

The asymptotic analysis of Crighton and Scott [14] tracks the development of the wave solution from a viscosity controlled shock up to an old-age linear decay phase. However, only the old-age solution has been compared with numerical results [8, 22]. While this does partially validate the full asymptotic analysis, the predictions of crucial physical quantities such as shock over-pressure and rise-time have previously not been rigorously tested. In Section 2 the asymptotic analysis is briefly summarised with a full explanation given in Appendix A.1. We use a change of variables so that the shock is fixed at leading order. This considerably simplifies the asymptotic analysis compared with earlier approaches [14] and is a key feature of the present paper. In Section 3 an implicit numerical scheme with variable spatial mesh is described, with comparisons between the asymptotic and numeric results in Section 4, including shock over-pressure and rise-time.

Of particular interest is Section 4.1 where the comparison between the asymptotic and numeric results is presented in the weak shock theory regime. In order to present accurate comparisons, asymptotic expressions are derived for specific definitions of the shock width and centre which are easily found numerically. Comparison with numeric results is considerably improved by the inclusion of higher order terms, previously undetermined by asymptotic analysis. Another key result in the spherically spreading case is the validation of the asymptotic prediction that the internal shock structure changes before the breakdown of weak shock theory.

2. Asymptotic theory

We consider the governing equation for $U(X, T)$ in the form

$$\frac{\partial U}{\partial T} + U\frac{\partial U}{\partial X} = \epsilon G(T)\frac{\partial^2 U}{\partial X^2}, \tag{5}$$

where $G(T)$ is given by (4) with $T_0 = 1$. For the planar case, an exact solution for arbitrary initial conditions is available via the Cole–Hopf transform [16,17], while for the cylindrical and spherical cases no general solutions are available. However, for many practical purposes (e.g. propagation of sonic booms through the atmosphere) the coefficient ϵ, which characterises the effect of thermoviscosity, is small which then allows asymptotic analysis. Typical numerical values for ϵ are discussed in Section 5.

For an initial disturbance, $U(X, 1)$, which is an odd function of X with $U \to 0$ as $|X| \to \infty$, nonlinear wave steepening leads to the appearance of a shock at some finite time and then weak shock theory predicts that the disturbance takes on the form of an N-wave at later times. Of prime importance is the range of validity of the N-wave with embedded shock and the particular shock structure, and this is the purpose of the present paper.

Rather than using the method of characteristics to analyse the evolution of the solution up to the formation of the N-wave, we choose to take a unit N-wave as the initial condition

$$U(X, 1) = \begin{cases} X, & \text{if } |X| < 1, \\ 0, & \text{otherwise,} \end{cases} \tag{6}$$

and then ignore the embryo shock region in which the discontinuity is resolved into a viscosity controlled shock.

2.1. Weak shock theory

Solving (5) subject to initial condition (6) for $\epsilon \ll 1$, weak shock theory predicts an N-wave with shocks located at $X = \pm T^{1/2}$ with corresponding amplitudes $\pm T^{-1/2}$. These embedded shocks are controlled by thermoviscosity and the structure of these shocks can be obtained directly from the asymptotic analysis of Crighton and Scott [14]. However rather than reproducing these results, we choose to present a condensed analysis in terms of new variables,

$$x = T^{-\frac{1}{2}}X, \qquad u = T^{\frac{1}{2}}U, \qquad t = \ln T.$$

This rescaling results in weak shock theory predicting a static, unit N-wave which will highlight any small changes of the shock structure, therefore making analysis of the shock simpler. The change of time variable is of lesser importance and chosen merely to simplify the governing equation to be solved numerically.

Please cite this article in press as: J.M. Schofield, P.W. Hammerton, Numerical and asymptotic solutions of generalised Burgers' equation, Wave Motion (2014), http://dx.doi.org/10.1016/j.wavemoti.2014.03.005

In terms of these new variables, the generalised Burgers' equation (5) reduces to

$$u_t = \frac{u}{2} + \left(\frac{x}{2} - u\right) u_x + \epsilon g(t) u_{xx}, \qquad g(t) = \begin{cases} 1 & \text{Plane} \\ \frac{1}{2}\exp(t) & \text{Cylindrical} \\ \exp(\exp(t)) & \text{Spherical} \end{cases} \tag{7}$$

which will now be referred to as the modified general Burgers' equation. Taking the unit N-wave as the initial condition, the outer solution then becomes

$$u(x,0) = \begin{cases} x, & \text{if } |x| < 1, \\ 0, & \text{otherwise,} \end{cases} \tag{8}$$

and we focus on the shock structure around $x = 1$. (Note that since the solution is anti-symmetric, the shock at $x = -1$ does not need a separate analysis.) Results can be obtained from the asymptotic analysis of Crighton and Scott and then expressed in terms of the new variables, but the direct analysis of (7) is in fact simpler and, for this reason, the analysis is summarised in Appendix A.1. The discontinuity in the outer solution at $x = 1$ is resolved by the introduction of a Taylor shock region [23], in which we find the following expression for the inner solution, where the inner variable $\hat{x} = (x-1)/\epsilon$ and the correction term $\epsilon\hat{v}$ is given in Appendix A.1.

$$u_{\text{in}}(\hat{x}, t) = \frac{1}{2}\left[1 - \tanh\left(\frac{\hat{x} + \int g(t)}{4g(t)}\right)\right] + \epsilon\hat{v} + O(\epsilon^2). \tag{9}$$

Hence, in terms of the outer variable x

$$u(x,t) = \frac{1}{2}\left[1 - \tanh\left(\frac{x - (1 - \epsilon\int g(t))}{4\epsilon g(t)}\right)\right] + \epsilon\hat{v} + O(\epsilon^2), \tag{10}$$

where the leading-order term represents a shock centred approximately at $x = 1 - \epsilon\int_0^t g(\tau)d\tau$ with width $O(\epsilon g)$.

Having found the general form for the shock, the next step is to look if this form will break down. The hyperbolic tangent shock can break down in three possible ways:

- The shock moves far away from its original location (i.e. $\epsilon\int g(t) = O(1)$);
- The shock width is no longer small compared to the size of the N-wave (i.e. $\epsilon g(t) = O(1)$);
- The leading order asymptotic solution is no longer significantly larger than the next order correction term $\epsilon\hat{v}$. In Appendix A.1 it is shown that this occurs when any one of $\epsilon\int g(t)$, $\epsilon g(t)$, $\epsilon g'(t) = O(1)$.

For the planar case, the breakdown first occurs when $t = O(\epsilon^{-1})$ due to the movement of the shock location and the leading order asymptotic solution no longer being valid. In the cylindrical case all three conditions are violated when $t = O(\log(\epsilon^{-1}))$. In the spherical case the breakdown first occurs when the hyperbolic tangent solution is no longer valid as the leading-order description. This occurs when $t = O(t_1)$, where

$$\epsilon\exp(t_1)\exp(\exp(t_1)) = 1, \tag{11}$$

at which point the shock is still relatively narrow and centred around $x = 1$. Thus the spherical case is different in that weak shock theory is still valid after the first breakdown and asymptotic analysis is possible at larger times. This is detailed in Appendix A.2.

While similar asymptotic expressions have been developed elsewhere [14], little work has been done on numerically verifying these results. In Section 4 we attempt to verify the asymptotic predictions by comparing them to the numerical solution of Burgers' equations in each case, focusing on the internal shock structure and the time-scales at which breakdown occurs. However, before this, we consider the asymptotic solutions valid for large time as another basis for comparison with numerical results.

2.2. Old age behaviour

Starting from the generalised Burgers' equation (5) in terms of X and T, the results of weak shock theory show that the maximum of U decreases as T increases. Hence, if we assume that $U \to 0$ as $T \to \infty$, then we can ignore the nonlinear effects, giving us the following PDE to solve,

$$U_T = \epsilon G(T) U_{XX}. \tag{12}$$

By inspection, a similarity solution can be obtained of the form

$$U(X,T) = Y(y)\Gamma(T), \quad y = \frac{X}{\left(\epsilon\int G dT\right)},$$

Please cite this article in press as: J.M. Schofield, P.W. Hammerton, Numerical and asymptotic solutions of generalised Burgers' equation, Wave Motion (2014), http://dx.doi.org/10.1016/j.wavemoti.2014.03.005

where

$$\Gamma(T) = \left(\int GdT\right)^{-A}, \qquad Y'' + \frac{y}{2}Y' - AY = 0. \tag{13}$$

The value of the separation constant A is found by noting that the equation for $Y(y)$ can be recast as a Hermite equation by letting $Y(y) = \exp(-\eta^2)f(\eta)$, where $\eta = y/2$. Since solutions exponentially growing in y are not physically realistic, we are restricted to negative values for A, while the condition $Y(0) = 0$ restricts us to integer values of A. As we are interested in the large time limit, the slowest decaying solution corresponds to $A = -1$, in which case $Y(y) = Cye^{-\frac{y^2}{4}}$, and the old-age solution takes the form

$$U(X,T) = D_j\left(\frac{X}{\left(\int G\right)^{\frac{3}{2}}}\right)\exp\left(-\frac{X^2}{4\epsilon\int GdT}\right), \tag{14}$$

where $j = 0, 1$ or 2 corresponding to the planar, cylindrical and spherical cases respectively. The coefficient D_j is a function of ϵ and depends on the nonlinear evolution from the initial condition and must be determined separately for the planar, cylindrical and spherical cases. For the planar case, where an exact solution is available through the Cole–Hopf transformation, the dependence of the old-age solution on X and T can be verified and the value of D_0 can be extracted from the exact solution to be $\exp(1/4\epsilon)$. For the cylindrical case Enflo [24] estimates D_1 through an innovative technique of matching the tail region of the shock (controlled by linear terms) through to the main shock region. For the spherical case D_2 was determined by Crighton and Scott [14] using the fact that the evolutionary shock described in Appendix A.2 acts as a matching region between the nonlinear regime and the old-age linear regime. The comparison between these predictions and the numerical solutions will be presented in Section 4.2.

3. Numerical schemes

There are a variety of possible schemes to use in order to generate a numerical solution to Burgers' equation. A commonly used numerical approach to the solution of nonlinear wave equations is the pseudospectral scheme [25]. Spatial derivatives are evaluated in spectral space, while the nonlinear term is evaluated in physical space and the solution is advanced forward in time in physical space. This approach has been successfully taken in the previous work when the main focus was on determining the old-age solution [22,26]. An advantage of this technique is that near discontinuities in the spatial profile at early times are successfully handled, without the need for fine resolution of the shock structure.

However, in the present work we also focus on validating the asymptotic structure of the shock at interim time scales. This requires fine resolution of the narrow shock region which, in spectral space, means that N, the number of spectral components which must be retained in a pseudospectral scheme, is unfeasibly large. Moreover, in the standard pseudospectral implementation, where the solution is advanced forwards in time via a Taylor series, the stability criterion takes the form $\Delta t < C/N^2$, where C is a constant and Δt is the time-step. Thus combining sufficient spatial resolution with wave evolution over long time scales is computationally expensive. For this reason we chose to use an implicit finite difference scheme with variable spatial mesh rather than a pseudospectral scheme.

An advantage of the formulation introduced in Section 2 is that in terms of the new variables, weak shock theory predicts a shock centred at $x = 1$ with unit amplitude. Thus in a variable mesh finite difference scheme the location where a fine mesh is required is known and asymptotic theory predicts the width of this region. However, it was seen in Section 2 that asymptotic theory predicts that the shock centre moves slightly over long periods. For this reason we incorporated mesh refinement into the numerical scheme, though the technique of changing variables so as to fix the shock location (at leading order) does mean that the frequency of mesh refinement required is much reduced.

In this paper a variable mesh scheme is used based on the method of Chong [19] which allows us to concentrate mesh points at the shock's location giving greater resolution of the shock whilst minimising the computational times.

Taking a Taylor series for $u_{i-1} = u(x_{i-1}, t)$ about $x = x_i$, we arrive at

$$u_{i-1} = u_i - h_i u_{i,x} + \frac{h_i^2}{2!}u_{i,xx} - \frac{h_i^3}{3!}u_{i,xxx} + \frac{h_i^4}{4!}u^-_{i,xxxx}, \tag{15}$$

where $u_i = u(x_i)$, $h_i = x_i - x_{i-1}$, $u_{i,x}$ is the first partial derivative evaluated at $x = x_i$ and u_i^- is evaluated at some point $x_{i-1} \le x \le x_i$. By obtaining a similar expression for u_{i+1} we arrive at the following expressions for u_x at $x = x_i$,

$$u_{i,x} = \Delta_x u_i - \frac{h_i h_{i+1}}{3!}u_{i,xxx} + \frac{h_i h_{i+1}}{4!(h_i + h_{i+1})}(h_i^2 u^-_{i,xxxx} - h_{i+1}^2 u^+_{i,xxxx}), \tag{16}$$

where $\Delta_x u_i$ is defined by

$$\Delta_x u_i = \frac{-h_{i+1}^2 u_{i-1} - (h_i^2 - h_{i+1}^2)u_i + h_i^2 u_{i+1}}{h_i h_{i+1}(h_i + h_{i+1})}.$$

Please cite this article in press as: J.M. Schofield, P.W. Hammerton, Numerical and asymptotic solutions of generalised Burgers' equation, Wave Motion (2014), http://dx.doi.org/10.1016/j.wavemoti.2014.03.005

By similar analysis we arrive at the following expression for the second derivative,

$$u_{i,xx} = \Delta_{xx}u_i - \frac{h_{i+1}-h_i}{3}u_{i,xxx} - \frac{h_{i+1}^3 u^+_{i,xxxx} + h_i^3 u^-_{i,xxxx}}{12(h_i+h_{i+1})}, \tag{17}$$

where $\Delta_{xx}u_i$ is defined by

$$\Delta_{xx}u_i = \frac{h_{i+1}u_{i-1} - (h_i+h_{i+1})u_i + h_i u_{i+1}}{h_i h_{i+1}(h_i+h_{i+1})/2}.$$

If the last two terms in (16) and (17) are relatively small we have that

$$u_{i,x} \approx \Delta_x u_i \quad \text{and} \quad u_{i,xx} \approx \Delta_{xx}u_i, \tag{18}$$

which can then be used as numerical approximations. In order to keep the last two terms in (16) and (17) relatively small we require h_i to be small in the shock regions, whereas in the smooth regions we can afford a coarser mesh. Also, the $(h_{i+1}-h_i)$ term in (17) indicates that we need to make a gradual change from a fine mesh to a coarse mesh.

The governing wave equation (7) is then solved using an implicit scheme. The advantage of this scheme is the improved stability criterion, $\Delta t < C(\Delta x)_{\text{Min}}$, rather than $\Delta t < C(\Delta x)^2_{\text{Min}}$ of the explicit scheme.

As described in Section 2, the solution of (7) involves a shock of unit amplitude centred at approximately $x = 1$ and hence we use a spatial mesh with a fine structure around $x = 1$. We define a variable mesh with the step size varying from $h = 0.01$ for the outer solution to $h = 0.01/\max|u_x|$ for the centre of the shock with a gradually changing mesh in between the two regions. Also, when the shock centre moves by a significant amount we can re-zone the mesh using a cubic spline interpolation scheme. The semi-infinite space, $x > 0$, is approximated by the region $[0, a]$ where a is the smallest value such that $u(a, t) < 10^{-8}$.

Before this numerical scheme is used to make comparisons with the asymptotic predictions, some method of validation is required. For the planar case we can use the Cole–Hopf transformation and solve Burgers' equation for arbitrary initial conditions. We took the unit N-wave (6) as the initial condition with a narrow smoothing region at $x = 1$. Comparison between the exact solution and the numerical solution was performed with $\epsilon = 0.001$, showing excellent agreement both in the overall waveform and the shock thickness. The agreement held for a range of different initial conditions.

4. Validation of asymptotic results

The motivation for developing a numerical scheme for the modified general Burgers' equation (7) is to verify the asymptotic predictions of Section 2, both when weak shock theory holds and in the old-age regime. We consider comparisons in both regimes for the cases of plane, cylindrical and spherical spreading waves.

4.1. Weak shock theory regime

First of all, we look at the times when the solution consists of an N-wave with an embedded shock. Using a composite expansion to combine the inner and outer solutions, an asymptotic prediction of the whole waveform can be obtained. These waveforms can be compared with numeric results and show excellent agreement until the asymptotic description begins to breakdown as outlined in Section 2. The relative difference between the asymptotic description and numerical waveform depends on the precise way in which the composite description is constructed. For this reason, we instead focus on the location of the shock centre and the shock width as a means of validating the asymptotic analysis. The best means of comparison between the numerical and asymptotic solutions is by considering the location of the shock centre and shock width for various times. From (10) our basic asymptotic predictions are that the shock is located at $1 - \epsilon\int g(t)$ and the shock width will behave like $4\epsilon g(t)$. However, in order to make quantitative comparisons between numerical solutions and the asymptotic descriptions of Section 2, a formal definition of shock centre and width is required. We define the shock width, x_{w}, to be the range within the shock over which the solution decreases from 90% of its maximum value to 10% of the maximum. The location of the shock centre, x_{m} is defined as the x position within the shock at which the amplitude is 50% of its maximum value.

This means that the asymptotic expression for the shock width needs to be revised in accordance with this definition of the width. This can be accomplished by deriving a perturbation expansion for the shock width and centre. In Appendix B we derive perturbation expansions for the shock width and location which also allow us to obtain first order correction terms for the shock width (B.6),

$$x_{\text{w}} = 8\alpha\epsilon g(t)\left(1 - 4\beta\epsilon g(t)\log\left(\frac{1}{2\epsilon g(t)}\right)\right) + O(\epsilon^2), \tag{19}$$

where $\alpha \approx 1.10$, and $\beta \approx 1.01$, and shock location (B.7),

$$x_{\text{m}} = 1 - \epsilon\int g(t) + 8(\epsilon g(t))^2\log\left(\frac{1}{2\epsilon g(t)}\right) + O(\epsilon^2), \tag{20}$$

Please cite this article in press as: J.M. Schofield, P.W. Hammerton, Numerical and asymptotic solutions of generalised Burgers' equation, Wave Motion (2014), http://dx.doi.org/10.1016/j.wavemoti.2014.03.005

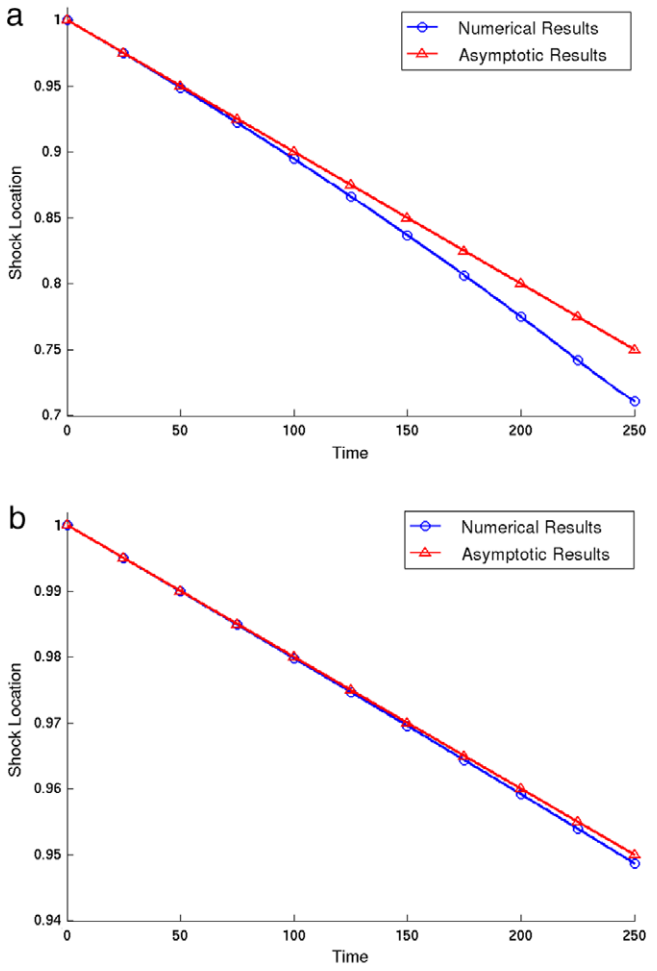

Fig. 1. Location of shock centre from numerical results compared to asymptotic predictions for the planar case with (a) $\epsilon = 0.001$; and (b) $\epsilon = 0.0002$.

valid when the shock takes the Taylor form (10). Including the next order correction to the shock only affects the $O(\epsilon^2)$ term in the expansions (19) and (20). These results can now be validated with a comparison between the numerical and asymptotic results. For the cylindrical and spherical cases we base the comparison on the shock width as this is the quantity of most physical interest. However for the planar case it is found that, at leading order, the shock width does not depend on time and hence we focus on the predictions of the location of the shock centre.

4.1.1. Planar case

In the planar case we have that $g(t) = 1$, and so the perturbation expansions for the shock location, x_m, and width, x_w, take the form

$$x_m = 1 - a_m\epsilon + b_m\epsilon^2, \quad a_m = t, \qquad b_m = 8\log\left(\frac{1}{2\epsilon}\right), \tag{21}$$

$$x_w = a_w\epsilon(1 - b_w\epsilon), \qquad a_w = 8\alpha, \quad b_w = 4\beta\log\left(\frac{1}{2\epsilon}\right). \tag{22}$$

Considering the expression for the shock width, x_w, it can seen that the first two terms in the perturbation expansion of the shock width are independent of time. After the initial embryo shock region, good agreement is seen between the numerical results and this constant value, with evidence that the shock width grows as $\epsilon^2 t$. This behaviour could feasibly be extracted from the second order correction term but is beyond the scope of this paper.

A more rigorous test of the validity of the asymptotic analysis comes from considering the shock location shown in (21). Comparisons between the numerical and asymptotic solutions for the shock location are shown in Fig. 1 for $\epsilon = 0.001$ and $\epsilon = 0.0002$. For these parameter values, the logarithmic correction term is sufficiently small that its inclusion cannot be seen in the plots. Excellent agreement is seen between the numerical and asymptotic solutions, with the asymptotic

Please cite this article in press as: J.M. Schofield, P.W. Hammerton, Numerical and asymptotic solutions of generalised Burgers' equation, Wave Motion (2014), http://dx.doi.org/10.1016/j.wavemoti.2014.03.005

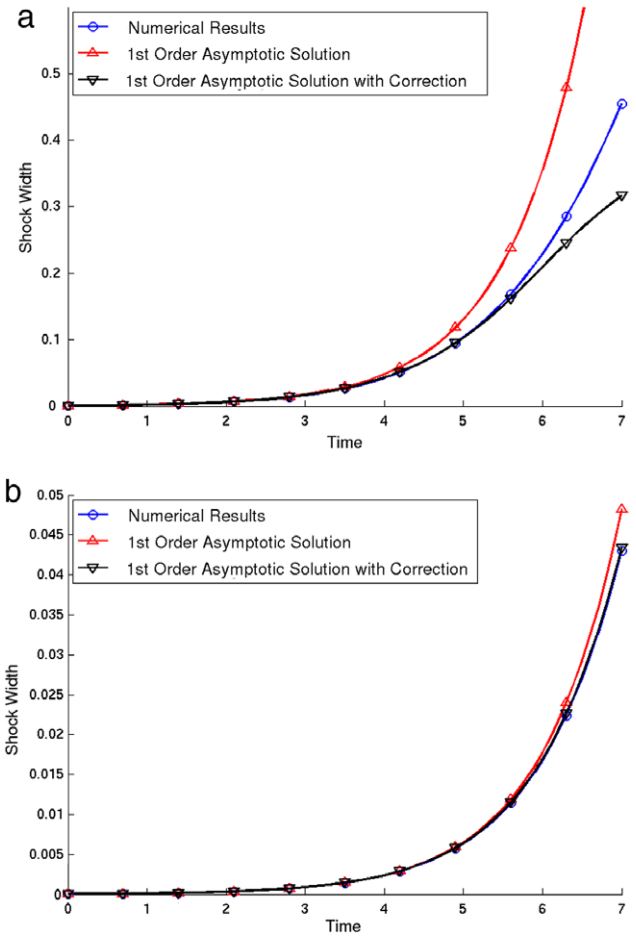

Fig. 2. A comparison of the shock width from numerical results and asymptotic predictions for the cylindrical case with $\epsilon = 0.0002$ (a); and $\epsilon = 0.00001$ (b).

prediction only diverging from the numerical results when the displacement of the shock centre from weak shock theory is no longer small.

To quantify this, we consider the time, t_*, at which the difference between the asymptotic and numerical predicted results for the shock centre is 0.1% and compare this with the timescale for the breakdown of the asymptotic solution obtained in Section 2 as ϵ^{-1}. For $\epsilon = 0.001$ we find $t_* = 46 = 0.046\epsilon^{-1}$, whereas when $\epsilon = 0.0002$, $t_* = 215 = 0.043\epsilon^{-1}$.

4.1.2. Cylindrical case

In the cylindrical case we have that $g(t) = \frac{1}{2}\exp(t)$, resulting in the following expressions for x_{m} and x_{w}

$$x_{\mathrm{m}} = 1 - a_{\mathrm{m}}\epsilon + b_{\mathrm{m}}\epsilon^2, \quad a_{\mathrm{m}} = \frac{1}{2}\left(e^t - 1\right), \quad b_{\mathrm{m}} = 2e^{2t}\log\left(\frac{1}{\epsilon e^t}\right), \tag{23}$$

$$x_{\mathrm{w}} = a_{\mathrm{w}}\epsilon(1 - b_{\mathrm{w}}\epsilon), \qquad a_{\mathrm{w}} = 4\alpha e^t, \qquad b_{\mathrm{w}} = 2\beta e^t\log\left(\frac{1}{\epsilon e^t}\right). \tag{24}$$

Comparisons between the asymptotic prediction for the shock width and numerical solutions are presented in Fig. 2 for two different values of ϵ. Considering only the leading order term in (24), Fig. 2 provides good evidence that the shock structure (10) is valid, but including the logarithmic correction term in the perturbation expansion significantly improves the agreement with numerical results. In particular, in Fig. 2(a), where $\epsilon = 0.0002$, we have good agreement between the numerical results and the leading-order asymptotic prediction up to $t \approx 3.7$ while including the logarithmic correction term increases the regime of agreement up to $t \approx 5.2$. At this time, the shock width is approximately 20% of the overall wave length, a point at which we would expect weak shock theory to be breaking down. In Fig. 2(b), where $\epsilon = 0.00001$, comparisons are included over the same time range, and at $t = 7$ the percentage error of the leading order asymptotic prediction and the numerical result is 12% while including the logarithmic correction reduces this error to 1%.

Please cite this article in press as: J.M. Schofield, P.W. Hammerton, Numerical and asymptotic solutions of generalised Burgers' equation, Wave Motion (2014), http://dx.doi.org/10.1016/j.wavemoti.2014.03.005

4.1.3. Spherical case

In the spherical case we have that $g(t) = \exp(\exp t)$, giving

$$x_m = 1 - a_m\epsilon + b_m\epsilon^2, \quad a_m = \mathrm{Ei}(e^t), \quad b_m = 2e^{2e^t}\log\left(\frac{1}{2\epsilon e^{e^t}}\right), \tag{25}$$

$$x_w = a_w\epsilon(1 - b_w\epsilon), \qquad a_w = 8\alpha e^{e^t}, \quad b_w = 4\beta e^{e^t}\log\left(\frac{1}{2\epsilon e^{e^t}}\right), \tag{26}$$

as the location and width of the Taylor-type shock, where $\mathrm{Ei}(x)$ is the exponential integral. Before we present the comparison between these asymptotic predictions and the numerical solutions, we recall from Section 2 that in the spherical case the breakdown of the tanh shock solution (10) occurs when it is no longer the leading order solution of (7). This occurs when $t = O(t_1)$, where t_1 is defined in (11). However, we still have a narrow shock centred around $x = 1$ and at larger times the composite asymptotic solution then takes the form

$$u(x, t) = \frac{x}{2}\mathrm{erfc}\left(\frac{x-1}{\sqrt{4\epsilon e^{e^t}/e^t}}\right), \tag{27}$$

where a full analysis is given in Appendix A.2. In order to compare this asymptotic prediction of shock width with the numerical solution of the full PDE (7), we follow the method described in Appendix B. At leading order, the shock width is given by $A\sqrt{\epsilon e^{e^t}/e^t}$, with A an order one constant determined numerically from the erfc function. The first order correction term is also obtained, however it turns out that the two-term perturbation expansion is only a useful approximation for extremely small values of ϵ and, as such, is not presented here. Instead, we determine the shock width numerically from the asymptotic solution (27) in the same way that the width is obtained from the full numerical solution, as described in Section 4.1. Thus we have two separate predictions from the asymptotic analysis to be compared with the full numerical solutions. For smaller times we have the Taylor shock width (26), whereas for larger times we have the shock width obtained from the error function shock form (27).

Comparisons between the asymptotic predictions and numerical solutions are presented in Fig. 3 for $\epsilon = 0.0005$ and $\epsilon = 0.00005$. In each case the width extracted from the full numerical solution is plotted alongside the leading-order result for the Taylor shock, the two-term Taylor result including the logarithmic correction term, and the width of the error function shock.

For Fig. 3(a), where $\epsilon = 0.0005$, we have good agreement between the numerical results and the first order asymptotic prediction until $t \approx 0.5$ and the correction to the asymptotic prediction increases the agreement until $t \approx 1.2$. For $t > 1.8$, agreement is seen between the numerical result and the width of the error function shock. The time, t_1, at which the shock structure is predicted to change from a hyperbolic tangent to an error function form is given by (11) and for $\epsilon = 0.0005$ this gives $t_1 \approx 1.76$.

For Fig. 3(b), where $\epsilon = 0.00005$, we again have excellent agreement between the asymptotic and numerical results with the transition between hyperbolic tangent shock form and the error function shock occurring in the region $1.7 < t < 2.1$ in agreement with the asymptotic scaling $t_1 \approx 2.06$. Hence the comparisons provide convincing validation of one of the most subtle aspects of the asymptotic analysis.

4.2. Old age solutions

As an additional verification of the asymptotic analysis, we also consider the old-age linear decay regime, though results are not presented for the planar case as exact solutions are available. The numerical approach described in Section 3 was taken until the shocks were relatively wide and there is no longer any need for a variable mesh. At this point a rescaling was made in order to allow easier comparison between the asymptotic old age form and the long time numerical results.

4.2.1. Cylindrical case

Guided by the old-age form (14) we choose the new variables $\bar{X} = X/T$, $\bar{T} = \ln T$ and $\bar{U} = UT^2$, so that the old age solution takes the form,

$$\bar{U} = D_1 f_1(\bar{X}), \qquad f_1(\bar{X}) = \bar{X}\exp\left(-\frac{\bar{X}^2}{\epsilon}\right), \tag{28}$$

where the constant D_1 depends on the nonlinear evolution from the specified initial condition. In terms of the new variables the GBE becomes

$$\bar{U}_{\bar{T}} = 2\bar{U} + \left(\bar{X} - \frac{\bar{U}}{e^{2\bar{T}}}\right)\bar{U}_{\bar{X}} + \frac{\epsilon}{2}\bar{U}_{\bar{X}\bar{X}}, \tag{29}$$

and in solving this numerically we extend the numerical solutions of Section 4.1 to larger times. For large $\bar{T}$ the solution approaches the universal form (28) and, once this has occurred, D_1 can then be obtained by considering the maximum value of $\bar{U}/f_1$, excluding the region where $\bar{U} \ll 1$.

Please cite this article in press as: J.M. Schofield, P.W. Hammerton, Numerical and asymptotic solutions of generalised Burgers' equation, Wave Motion (2014), http://dx.doi.org/10.1016/j.wavemoti.2014.03.005

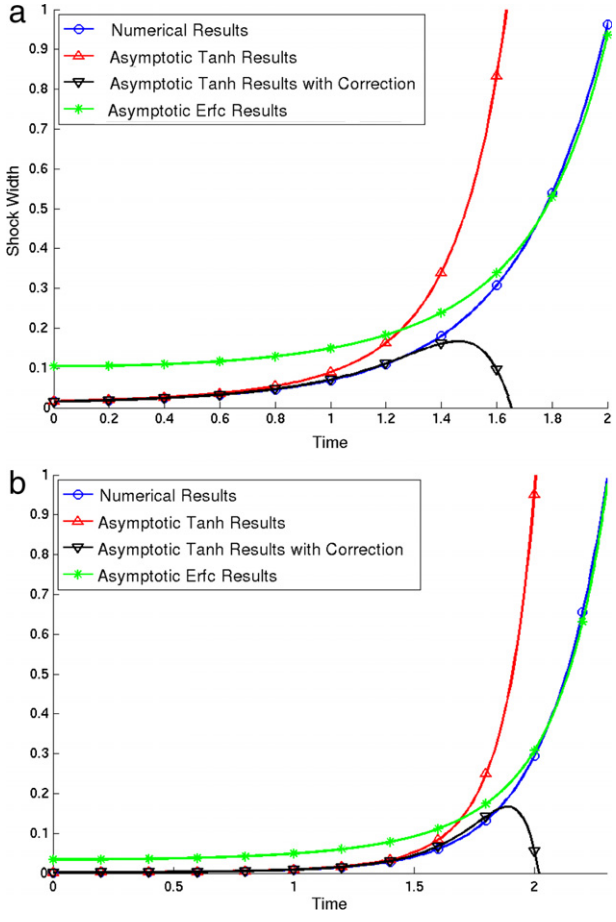

Fig. 3. A comparison of the shock width from the numerical results and asymptotic predictions for the spherical case with $\epsilon = 0.0005$ (a) and $\epsilon = 0.00005$ (b). This figure shows the progression from the tanh shock (26), to the erf shock (27).

The dependence of D_1 on ϵ is readily determined, at least at leading order, through the log–log plot of Fig. 4(a) and we see that D_1 varies as ϵ^{-2}. This dependence on ϵ is in agreement with the numerical results of Sachdev [8] and Hammerton and Crighton [9]. Numerical values for D_1 evaluated by the numerical scheme described above are compared with earlier results in Table 1. Note, the current scheme allows for much smaller values of ϵ to be considered than was possible with the earlier results.

Obtaining a quantitative prediction of D_1 has proved a challenge and 'its determination remains an important unsolved canonical problem of nonlinear acoustics' [14]. By considering the tail of the shock (which satisfies a linear equation) and matching to the main part of the shock, Enflo [24] was able to determine an approximation to the constant D_1, also presented in Table 1,

$$D_{\mathrm{E}} = \frac{1}{\epsilon^2}\frac{27}{16}\frac{1}{\sqrt{6\mathrm{e}}}\left[(1+2\epsilon) - \frac{1}{2}\left(1+\frac{8}{3}\epsilon\right)\left(\frac{\pi^2}{6} - \ln 2 - \frac{11}{36}\right)\right]. \tag{30}$$

It should be noted that this is not a perturbation expansion in small ϵ, rather the first two terms in a summation that is assumed to converge reasonably quickly. Due to algebraic complexity, obtaining subsequent terms in the summation is unrealistic. In order to assess the accuracy of (30) in Fig. 4(b) we plot D_1/D_{E} as a function of ϵ. Thus, it appears that the terms ignored in [24] contribute approximately 26% to the estimate of D_1.

4.2.2. Spherical case

For the spherical case we take a similar approach to that outlined above. We make the change of variables $\bar{X} = X/e^{-T/2}$, $\bar{T} = T$ and $\bar{U} = Ue^T$, so that the old-age form becomes

$$\bar{U} = D_2 f_2(\bar{X}), \qquad f_2(\bar{X}) = \bar{X}\exp\left(-\frac{\bar{X}^2}{4\epsilon}\right) \tag{31}$$

Please cite this article in press as: J.M. Schofield, P.W. Hammerton, Numerical and asymptotic solutions of generalised Burgers' equation, Wave Motion (2014), http://dx.doi.org/10.1016/j.wavemoti.2014.03.005

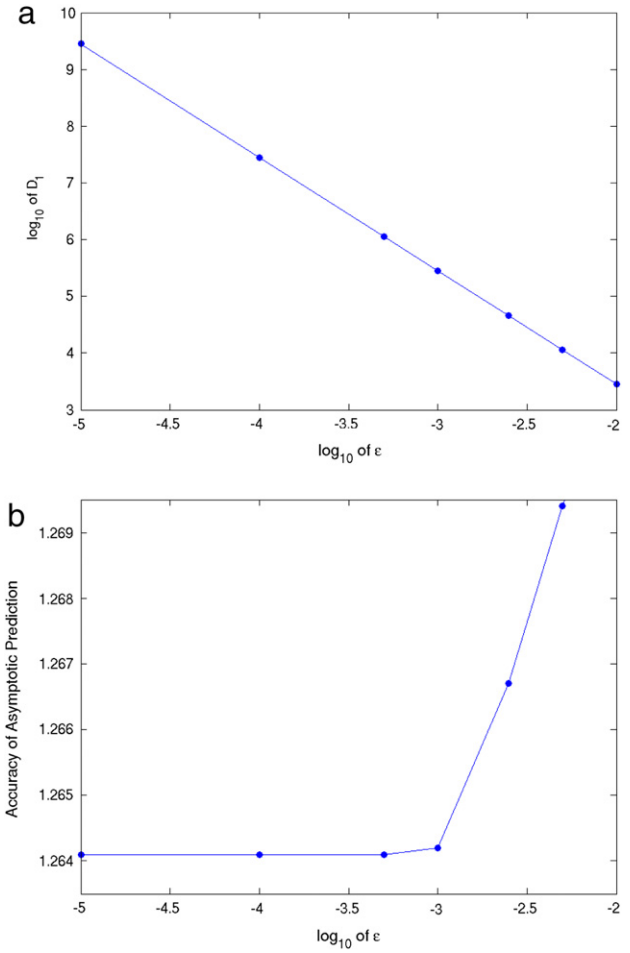

Fig. 4. The values of D_1 for various values of ϵ for the cylindrical case (a) and a comparison of the values of ϵ and the accuracy of the asymptotic predictions for the cylindrical case (b).

Table 1
A comparison of the results of determining D_1.

		ϵ				
		0.00001	0.0001	0.001	0.017	0.1
$\epsilon^2 D_1$	Present	0.36	0.36	0.36	0.37	0.44
	Hammerton & Crighton	–	–	0.35	0.37	0.43
	Sachdev	–	–	–	0.34	–
	Enflo (analytic)	0.28	0.28	0.28	0.29	0.33

with the GBE in terms of the new variables becoming,

$$\bar{U}_{\bar{T}} = \bar{U} + \left(\frac{\bar{X}}{2} - \frac{\bar{U}}{(e^{3\bar{T}/2})}\right)\bar{U}_{\bar{X}} + \epsilon \bar{U}_{\bar{X}\bar{X}}. \tag{32}$$

As for the cylindrical case, the numerical scheme of Section 3 was used for early times and then an equally spaced mesh was used to solve (32) and continue the numerical results for larger times until the old age solution was reached. A numerical value of D_2 is obtained by considering $\bar{U}/f_2$ as described for the cylindrical case. However, in contrast to the cylindrical case, an expression for D_2 can be obtained as a formal asymptotic limit [14], $D_2 = C^{\frac{1}{2}}/6\pi^{\frac{1}{2}}\epsilon^{\frac{3}{2}}$, where C is such that $\epsilon \exp(C)/C = 1$. Again we can plot the ratio of the asymptotic constant and the numerical constant as a function of ϵ. From Fig. 5 it is reasonable to conclude that as $\epsilon \to 0$, the numerical value of D_2 approaches the asymptotic approximation of Crighton and Scott [14], though close agreement is only obtained for very small values of ϵ.

Please cite this article in press as: J.M. Schofield, P.W. Hammerton, Numerical and asymptotic solutions of generalised Burgers' equation, Wave Motion (2014), http://dx.doi.org/10.1016/j.wavemoti.2014.03.005

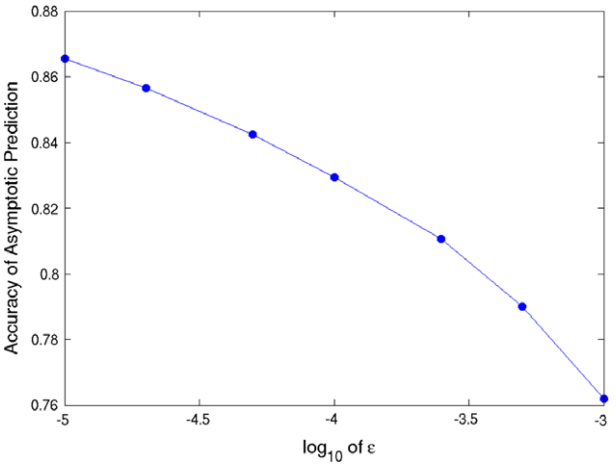

Fig. 5. A plot of the ratios of the asymptotic predictions to the numerical solutions for various values of ϵ for the spherical case.

5. Summary

In this paper we have considered solutions of the generalised Burgers' equation relevant to a pressure pulse travelling in one-dimension, or spreading subject to cylindrical or spherical symmetry. When the dimensionless viscosity is small, an in-depth asymptotic analysis is possible, and this is summarised in Section 2. In each geometric case a shock forms and the internal structure of the shock is determined. As the wave evolves, the amplitude decreases, the shock widens and, in the case of spherical spreading, it changes its internal form. Compared to earlier work, the present formulation involving a novel change of variables simplifies the description of the shock form. In addition, precise definitions of the shock width and the position of the shock centre are provided so that the asymptotic predictions are obtained in a form which is much more amenable to comparisons with numerical results and experimental measurements.

Pseudospectral schemes have traditionally been used for solving generalised Burgers' equation, but since we are interested in the internal shock structure to the same degree as the overall waveform, we choose to use a variable mesh finite difference scheme and this is described in Section 3. Key to the success of this scheme is the change of variables previously described which keeps the shock fixed at leading order and so reduces the need for redefining the mesh.

In each geometric case the asymptotic analysis predicts a timescale at which weak shock theory breaks down. Only as we approach this time do we see the numeric waveform diverge from the composite expansion of the waveform. Rather than focus on the differences between the overall waveform and the numerical solution for various values of ϵ, which is complicated by the fact that the key timescales are also functions of ϵ, we focus on the shock location and shock width. This proves to be a more rigorous check of the asymptotics. In Figs. 1–3 these asymptotic predictions are verified by comparison with numerical results. Also worth noting is the next order correction term for the shock's location and width presented in Figs. 2 and 3 which offers a new level of accuracy in determining these quantities and further validates the asymptotic approach. Another key result is that of Fig. 3 where it is seen that the subtle change in shock structure and resulting change in shock width predicted asymptotically is a genuine phenomenon and may be relevant to measurements of rise time for sonic booms.

For large times (or equivalently large propagation distances) the waveform approaches an old-age regime with linear decay. Though the results in this regime are of less physical relevance, much interest has previously been focused on the amplitude of these linear solutions. The comparisons with numeric results presented in Figs. 4(b) and 5 go some way to validating the theoretical predictions of the old-age form. In particular the approach taken by Enflo [24] seems justified though additional terms would be needed to improve the accuracy of the old-age amplitude prediction.

Results presented show that agreement between asymptotic predictions and numerical results is only good for very small values of ϵ. However, by considering the parameters of a typical sonic boom, it can be seen that these values of small ϵ are relevant to physical situations. For example, considering a disturbance generated by a supersonic aircraft will result in a typical sound pressure level of around 140 dB, which corresponds to a peak overpressure of 200 Pa. From here, we can find the disturbance velocity of the air molecules to be $U_0 \approx 0.5$ m s^{-1} and for a sound pressure level >120 dB, the diffusivity of sound is $\Delta \approx 1.9 \times 10^{-5}$ m^2 s^{-1}. For a small aircraft travelling at supersonic speeds a mach cone is produced which is approximately cylindrically symmetric and with a distance between head shock and tail shock of $l_0 \approx 10$ m. Combining all these values, along with the adiabatic exponent $\gamma \approx 1.4$, allows us to determine the coefficient of the thermoviscous dissipative term

$$\epsilon = \frac{2\Delta}{(\gamma+1)U_0 l_0 T_0} \approx 3 \times 10^{-6}, \tag{33}$$

Please cite this article in press as: J.M. Schofield, P.W. Hammerton, Numerical and asymptotic solutions of generalised Burgers' equation, Wave Motion (2014), http://dx.doi.org/10.1016/j.wavemoti.2014.03.005

where we have set $T_0 = 1$ as described in Section 2. Note this value of ϵ is similar to that presented in Fig. 2(b) where $\epsilon = 1 \times 10^{-5}$ and there was good agreement between the asymptotic predictions and numerical results. Laboratory measurements for a spherically spreading shock generated by an electrical spark source [27] correspond to $\epsilon \approx 1 \times 10^{-3}$, which is similar to Fig. 3(a) where good agreement was found with $\epsilon = 5 \times 10^{-4}$.

In this paper we have demonstrated the value of asymptotic analysis for nonlinear wave problems and verified these predictions by comparison with numerical results (obtained by suitable rescaling and a variable mesh scheme). It has been shown that the parameter values used in this paper are of the same order as those caused by a disturbance generated by a supersonic aircraft at cruise conditions. In practice, other effects should also be considered for nonlinear propagation over long ranges through the atmosphere such as molecular relaxation, atmospheric stratification and meteorological conditions. However, in many cases these effects can be represented by additional linear terms leading to generalisations of Burgers' equation. Asymptotic analysis of these equations would then allow identification of the key physical processes and efficient parametric studies of rise time and over pressure. Not only does the present work go a long way towards validating such an approach, but the asymptotic approach described will also considerably simplify the analysis of the more complicated generalisations of Burgers' equation.

Acknowledgements

We thank the referees for their helpful comments on this paper.

Appendix A. Shock structure

A.1. Shock structure of modified general Burgers' equation

We consider the small ϵ-solution of the modified general Burgers' equation (7) with outer solution given by (8). Focusing on the shock centred at $x = 1$, we set $x = 1 + \epsilon\hat{x}$ and, in terms of the inner variable $\hat{x}$, (7) becomes

$$u_t = \frac{1}{\epsilon}\frac{\partial}{\partial \hat{x}}\left[\frac{1}{2}(u - u^2) + g(t)u_{\hat{x}} + \frac{1}{2}\epsilon\hat{x}u\right], \tag{A.1}$$

with matching conditions $u \to 0$ as $\hat{x} \to \infty$ and $u \to 1$ as $\hat{x} \to -\infty$. Writing $u = \hat{u} + \epsilon\hat{v} + O(\epsilon^2)$, at leading order we have

$$\frac{1}{2}(\hat{u} - \hat{u}^2) + g(t)\hat{u}_{\hat{x}} = 0, \tag{A.2}$$

with solution

$$\hat{u} = \frac{1}{2}\left(1 - \tanh\theta\right), \qquad \theta = \frac{\hat{x} + f(t)}{4g(t)}. \tag{A.3}$$

In order to determine $f(t)$, the next order term in the expansion for u must be considered. Recasting (A.1) in terms of θ and, after some manipulation, we obtain

$$u_t + \frac{ug'}{g} = \frac{1}{4g}\frac{\partial}{\partial\theta}\left[\left((2g + 4g')\theta - \frac{f}{2} - f'\right)u + \frac{1}{4\epsilon}\left(2(u - u^2) + u_\theta\right)\right]. \tag{A.4}$$

As before we substitute $u = \hat{u} + \epsilon\hat{v} + O(\epsilon^2)$ and $\hat{v}$ satisfies

$$\left((2g + 4g')\theta - \frac{f}{2} - f'\right)\hat{u} + \frac{1}{4}\left(2\hat{v} - 4\hat{u}\hat{v} + \hat{v}_\theta\right) = 4g'\left(\int \hat{u}d\theta\right). \tag{A.5}$$

Substituting $\hat{u} = \frac{1}{2}(1 - \tanh(\theta))$ then gives

$$\hat{v}_\theta + 2\hat{v}\tanh\theta = -(A\theta + B)(1 - \tanh\theta) - C(\ln(\cosh\theta) + \ln 2 - \theta), \tag{A.6}$$

where

$$A(t) = 4g + 8g', \qquad B(t) = -2f' - f, \qquad C(t) = 8g'. \tag{A.7}$$

Solving (A.6) we arrive at

$$\hat{v} = \frac{1}{8\cosh^2\theta}\left[K(t) + A(t)p_1(\theta) + B(t)p_2(\theta) + C(t)p_3(t)\right], \tag{A.8}$$

Please cite this article in press as: J.M. Schofield, P.W. Hammerton, Numerical and asymptotic solutions of generalised Burgers' equation, Wave Motion (2014), http://dx.doi.org/10.1016/j.wavemoti.2014.03.005

where

$$p_1(\theta) = (2\theta+1)e^{-2\theta} - 2\theta^2,$$
$$p_2(\theta) = 2e^{-2\theta} - 4\theta + 2,$$
$$p_3(\theta) = 2\theta\sinh(2\theta) - \mathrm{diln}\left(-e^{-2\theta}\right) - e^{-2\theta} - 2\sinh(2\theta)\ln(2\cosh(\theta)) - 2\theta,$$

with diln denoting the dilogarithm, $\mathrm{diln}(x) = -\int_1^x \frac{\log t}{t-1}dt$. $K(t)$ can be determined by considering the form of the governing equation at $O(\epsilon^2)$, as outlined by Crighton and Scott. However, it can be readily seen that it has no effect on the nature of the asymptotic breakdowns and hence we do not determine it explicitly using the present notation.

Matching to the outer solution, the condition $\hat{v} \to 0$ as $\theta \to \infty$ is automatically satisfied. Letting $\theta \to -\infty$ gives

$$\lim_{\theta\to-\infty}(\hat{v}) = \left(\theta+\frac{1}{2}\right)A + B - \left(\theta+\frac{1}{2}\right)C, \tag{A.9}$$

and hence using the values of A, B, and C from (A.7),

$$\lim_{\theta\to-\infty}\left(\hat{u}+\epsilon\hat{v}\right) = 1 + \epsilon\left(4g\theta + 2g - 2f' - f\right). \tag{A.10}$$

In terms of the inner variables, the outer solution is given by $u = 1 + \epsilon(4g\theta - f)$ and hence matching inner and outer solutions fixes

$$f = \int_0^t g(\tau)d\tau. \tag{A.11}$$

Finally inserting this result into Eq. (A.3) we get

$$u = \frac{1}{2}\left[1 - \tanh\left(\frac{x - \left(1 - \epsilon\int g(t)\right)}{4\epsilon g(t)}\right)\right] + \epsilon\hat{v}. \tag{A.12}$$

Moreover, for a given $g(t)$, the expression for $\hat{v}$ allows us to identify if $\epsilon\hat{v}$ becomes order one, in which case the Taylor solution is no longer valid as a leading order description of the embedded shock. From inspection of (A.8) it can be seen that $\epsilon\hat{v}$ becomes order one when any one of $\epsilon\int g(t)$, $\epsilon g(t)$, $\epsilon g'(t)$ becomes order one. The breakdown of the Taylor solution for the cases of plane, cylindrical and spherical waves is discussed in Section 2.

A.2. Spherical case — evolutionary shock structure

As observed in Section 2, the case of spherical spreading is qualitatively different from the planar and cylindrical cases in that, when the leading order solution breaks down, we still have a narrow shock region centred around $x = 1$. This breakdown occurs when $\epsilon e^{e^t}e^t = O(1)$.

In order to investigate the development of the shock structure, we introduce a new time variable t' defined by $e^{t'} = e^t - e^{t_1}$ where $\epsilon e^{e^{t_1}}e^{t_1} = 1$. This reduces the modified general Burgers' equation (10) to

$$u_{t'} = \frac{u}{2} + \left(\frac{x}{2} - u\right)u_x + e^{e^{t'}}e^{-t_1}u_{xx}. \tag{A.13}$$

By examination of the Taylor shock solution (A.12) valid for $t < t_1$, we apply the changes of variables, $u' = \sqrt{e^{t_1}}u - \frac{1}{2}$ and $x' = \sqrt{e^{t_1}}(x-1)$, and neglect any small shift in the shock location in line with the analysis of Crighton and Scott [14]. This reduces (A.13) to

$$u'_{t'} = \frac{u'}{2} + \left(\frac{x'}{2} - u'\right)u'_{x'} + e^{e^{t'}}u_{x'x'} + \frac{1}{4}, \tag{A.14}$$

leading to

$$u' = \frac{1}{2}\sqrt{e^{t'}}\left(\mathrm{erfc}\left(\frac{1}{2}\sqrt{\frac{e^{t'}}{e^{e^{t'}}}}x'\right) - 1\right), \tag{A.15}$$

which is the form the new shock takes and corresponds to result of (3.46) of Crighton and Scott [14]. In terms of the original variables, the inner solution becomes

$$u = \frac{1}{2}\mathrm{erfc}\left(\frac{x-1}{\sqrt{4\epsilon e^{e^t}/e^t}}\right), \tag{A.16}$$

corresponding to a shock whose width scales like $\sqrt{\epsilon e^{e^t}/e^t}$.

Please cite this article in press as: J.M. Schofield, P.W. Hammerton, Numerical and asymptotic solutions of generalised Burgers' equation, Wave Motion (2014), http://dx.doi.org/10.1016/j.wavemoti.2014.03.005

Appendix B. Shock width and shock centre

In Section 3 we defined the shock width, x_w, to be the x-range within the shock over which the solution decreases from 90% of its maximum value to 10% of its maximum. The location of the shock centre, x_m is defined as the x position within the shock at which the amplitude is 50% of the maximum value. Here we present asymptotic expansions for these quantities.

We consider the case when the shock takes the Taylor form (10), in which case the solution for $x > 0$ can be written in the composite form

$$f(x,t) = \frac{x}{2}\left(1 - \tanh\theta\right), \qquad \theta = \frac{x - (1-\epsilon a)}{\epsilon b}, \tag{B.1}$$

where $a = \int g(t)$ and $b = 4g(t)$. Letting $\hat{f}(t)$ be the maximum of $f(x,t)$ over $x > 0$, we define x_m, $x_{90\%}$ and $x_{10\%}$ as

$$f(x_{90\%},t) = 0.9\hat{f}, \qquad f(x_m,t) = 0.5\hat{f}, \qquad f(x_{10\%},t) = 0.1\hat{f}. \tag{B.2}$$

In order to calculate these values asymptotically in the small ϵ limit, we rewrite Eq. (B.1) in terms of θ

$$f(\theta,t) = \frac{1}{2}(1 - \epsilon a + \epsilon b\theta)(1 - \tanh\theta).$$

This function has a maximum value when $\theta = \hat{\theta}$, which is obtained by solving $\frac{\partial f}{\partial \theta} = 0$. Hence $\hat{\theta}$ satisfies

$$\frac{1}{\epsilon b} + \left(\frac{a}{b} + \hat{\theta}\right) = \frac{1}{2}(e^{-2\hat{\theta}} + 1).$$

In the limit $\epsilon \to 0$, the leading order term $\frac{1}{\epsilon b}$ must be balanced by the exponential term, hence $\hat{\theta} \approx -\frac{1}{2}\log B$, where $B = \left(\frac{2}{\epsilon b}\right)$. Noting that $\tanh(-\frac{1}{2}\log B) = (1-B)/(1+B)$, the maximum value of f is given by

$$\begin{aligned}\hat{f} &\approx \left[\left(1 - \epsilon a - \frac{\epsilon b}{2}\log(B)\right)\frac{1}{1+\frac{1}{B}}\right] \\ &\approx 1 - \epsilon\left(a - \frac{b}{2}\right) - \frac{1}{B}(\log(B)) + \mathrm{O}\left(\epsilon^2 \log\left(\frac{1}{\epsilon}\right)\right).\end{aligned}$$

Having found the location of the maximum value of f, we can now find the shock centre and width by solving

$$f(\theta_\lambda + \delta_\lambda) = \lambda\hat{f}, \tag{B.3}$$

where λ is a constant, θ_λ is the leading order solution in the small ϵ limit and δ_λ represents a small perturbation. Solving for $\lambda = 0.9, 0.5, 0.1$ then determines $x_{90\%}$, x_m and $x_{10\%}$ respectively. Taking the Taylor expansion about θ_λ and substituting for $\hat{f}$ gives

$$\frac{1}{2}(1 - \tanh(\theta_\lambda)) - \frac{1}{2}\delta_\lambda \operatorname{sech}^2\theta_\lambda + O(\epsilon) = \lambda - \frac{1}{2}b\lambda\epsilon\log B + O(\epsilon),$$

and hence,

$$\tanh(\theta_\lambda) = 1 - 2\lambda, \quad \text{and} \quad \delta_\lambda = \frac{b\lambda\epsilon\log B}{\operatorname{sech}^2\theta_\lambda} = \frac{b\epsilon\log B}{4(1-\lambda)}. \tag{B.4}$$

Solving for $\lambda = 0.1, 0.9$ we obtain

$$\theta_{0.1} = \alpha, \qquad \theta_{0.9} = -\alpha, \quad \text{where } \alpha = \tanh^{-1}(0.8) \approx 1.10,$$

and so

$$\begin{aligned}x_{10\%} &= 1 - \epsilon(a - \alpha b) + A_{10\%}\epsilon^2 b^2 \log B, \qquad A_{10\%} = \frac{1}{4\times 0.9}, \\ x_{90\%} &= 1 - \epsilon(a + \alpha b) + A_{90\%}\epsilon^2 b^2 \log B, \qquad A_{90\%} = \frac{1}{4\times 0.1}.\end{aligned} \tag{B.5}$$

Finally the shock width is given by

$$x_w = x_{90\%} - x_{10\%} = 2\alpha\epsilon b\left(1 - \beta\epsilon b\log\left(\frac{2}{\epsilon b}\right)\right) + O(\epsilon^2), \tag{B.6}$$

where

$$\beta = \frac{A_{90\%} - A_{10\%}}{2\alpha} \approx 1.01.$$

Please cite this article in press as: J.M. Schofield, P.W. Hammerton, Numerical and asymptotic solutions of generalised Burgers' equation, Wave Motion (2014), http://dx.doi.org/10.1016/j.wavemoti.2014.03.005

Considering the case $\lambda = 0.5$ we can find an expression for the centre of the shock. We have $\theta_{0.5} = 0$ and $\delta_{0.5} = \frac{1}{2}b\epsilon \log B$, and hence the shock is centred at

$$x_m = 1 - \epsilon a + \frac{1}{2}(\epsilon b)^2 \log\left(\frac{2}{\epsilon b}\right) + O(\epsilon^2). \tag{B.7}$$

Including the $O(\epsilon)$ correction to the inner solution (9), as described in Appendix A.1, only affects the $O(\epsilon^2)$ terms in (B.6) and (B.7) and hence this term can be safely ignored.

An alternative approach to finding the shock width and shock centre predicted by asymptotic theory is to solve (B.2) numerically. This was also done and showed excellent agreement with the expansions (B.6) and (B.7).

References

[1] J. Mendousse, Nonlinear dissipative distortion of progressive sound waves at moderate amplitudes, J. Acoust. Soc. Am. 25 (1953) 51.
[2] M. Lighthill, Viscosity effects in sound waves of finite amplitude, Surv. Mech. (1956) 250–351.
[3] L. Sirovich, T. Chong, Supersonic flight in a stratified sheared atmosphere, Phys. Fluids 17 (1974) 310–320.
[4] P. Blythe, Nonlinear wave propagation in a relaxing gas, J. Fluid Mech. 37 (1969) 31–50.
[5] H. Ockendon, D. Spence, Nonlinear wave propagation in a relaxing gas, J. Fluid Mech. 39 (1969) 329–345.
[6] P. Hammerton, Effect of molecular relaxation on the propagation of sonic booms through a stratified atmosphere, Wave Motion 33 (2001) 359–377.
[7] H.E. Bass, R. Raspet, J.P. Chambers, M. Kelly, Modification of sonic boom wave forms during propagation from the source to the ground, J. Acoust. Soc. Am. 111 (2002) 481.
[8] P. Sachdev, V. Tikekar, K. Nair, Evolution and decay of spherical and cylindrical N waves, J. Fluid Mech. 172 (1986) 347–371.
[9] P.W. Hammerton, D.G. Crighton, Old-age behavior of cylindrical and spherical nonlinear-waves — numerical and asymptotic results, Proc. R. Soc. Lond. Ser. A Math. Phys. Eng. Sci. 422 (1989) 387–405.
[10] F. Pestorius, D. Blackstock, Propagation of finite-amplitude noise, in: L. Bjorno (Ed.), Finite-Amplitude Wave Effects in Fluids, 1974, pp. 24–29.
[11] H. Bass, R. Raspet, Comparison of sonic boom rise time prediction techniques, J. Acoust. Soc. Am. 91 (1992) 1767.
[12] R. Cleveland, J. Chambers, H. Bass, R. Raspet, D. Blackstock, M. Hamilton, Comparison of computer codes for the propagation of sonic boom waveforms through isothermal atmospheres, J. Acoust. Soc. Am. 100 (1996) 3017–3027.
[13] R. Cleveland, M. Hamilton, D. Blackstock, Time-domain modeling of finite-amplitude sound in relaxing fluids, J. Acoust. Soc. Am. 99 (6) (1996) 3312–3318.
[14] D.G. Crighton, J.F. Scott, Asymptotic solutions of model equations in nonlinear acoustics, Roy. Soc. Lond. Philos. Trans. Ser. A 292 (1979) 101–134.
[15] M.E. Johnson, P.W. Hammerton, Effect of molecular relaxation processes on travelling wave solutions of sonic boom waveforms, Wave Motion 38 (3) (2003) 229–240.
[16] E. Hopf, The partial differential equation $u_t + uu_x = \mu u_{xx}$, Comm. Pure Appl. Math. 3 (3) (1950) 201–230.
[17] J.D. Cole, et al., On a quasi-linear parabolic equation occurring in aerodynamics, Quart. Appl. Math 9 (3) (1951) 225–236.
[18] J. Billingham, A. King, Wave Motion, Cambridge University Press, 2000.
[19] T. Chong, A variable mesh finite difference method for solving a class of parabolic differential equations in one space variable, SIAM J. Numer. Anal. 15 (4) (1978) 835–857.
[20] C. Basdevant, M. Deville, P. Haldenwang, J. Lacroix, J. Ouazzin, R. Peyret, P. Orlandi, A. Patera, Spectral and finite difference solutions of the burgers equation, Computers Fluids 14 (1986) 23–41.
[21] S. Leibovich, A.R. Seebass, Nonlinear Waves, Cornell University Press, 1974.
[22] P. Hammerton, D. Crighton, Old-age behaviour of cylindrical and spherical nonlinear waves: numerical and asymptotic results, Proc. R. Soc. Lond. Ser. A. Math. Phys. Sci. 422 (1863) (1989) 387–405.
[23] G.I. Taylor, The conditions necessary for discontinuous motion in gases, Roy. Soc. Lond. Proc. Ser. A 84 (1910) 371–377.
[24] B. Enflo, On the connection between the asymptotic waveform and the fading tail of an initial n-wave in nonlinear acoustics, Acta Acust. Unit. Acust. 84 (3) (1998) 401–413.
[25] B. Fornberg, A Practical Guide to Pseudospectral Methods, vol. 1, Cambridge Univ. Press, 1998.
[26] P. Sachdev, V. Tikekar, K. Nair, Evolution and decay of spherical and cylindrical n waves, J. Fluid Mech. 172 (1986) 347–371.
[27] P. Yuldashev, M. Averiyanov, V. Khokhlova, S. Ollivier, P. Blanc-Benon, Nonlinear spherically divergent shock waves propagating in a relaxing medium, Acoust. Phys. 54 (1) (2008) 32–41.

Please cite this article in press as: J.M. Schofield, P.W. Hammerton, Numerical and asymptotic solutions of generalised Burgers' equation, Wave Motion (2014), http://dx.doi.org/10.1016/j.wavemoti.2014.03.005